Terr. Atmos. Ocean. Sci., Vol. 27, No. 6, 819-824, December 2016 doi: 10.3319/TAO.2016.07.28.02

Taiwan Borehole Seismometer Application in Earthquake Early Warning

Po-Lun Huang, Ting-Li Lin *, Hao-Jen Hsiao, and Ruei-Hua Huang

Department of Earth Sciences, National Cheng Kung University, Tainan City, Taiwan, R.O.C.

Received 26 February 2016, revised 18 July 2016, accepted 28 July 2016

ABSTRACT

Earthquake early warning (EEW) is an effective approach to mitigating earthquake damage. This is the first study evaluating borehole seismograph application to EEW in Taiwan. We selected inland and offshore earthquakes with M_L larger than 4.0 occurring between 2012 and 2014 for this study. We investigated the P*d* attenuation relationship as a function of the hypocentral distance (R) and magnitude (M). The new P*d* attenuation relationship specific for the borehole records is expressed as: $\log(Pd) = 0.689M_L - 0.741\log(R) - 4.608 \pm 0.248$. Once the earthquake location is determined, this regression equation is used to quickly estimate P*d* magnitude (M_{Pd}). According to the new regression equation formulated specifically for borehole observations in Taiwan, our result shows that the standard M_{Pd} deviation is about 0.21 relative to M_L. This smaller standard deviation of 0.21 compared to that of the free-surface records might be attributed to the reduced influence of near-surface effects in the borehole records. We propose a new robust P*d* regression equation for the Taiwan borehole seismic network.

Key words: Earthquake early warning, Borehole seismometer, P*d* magnitude

Citation: Huang, P. L., T. L. Lin, H. J. Hsiao, and R. H. Huang, 2016: Taiwan borehole seismometer application in Earthquake Early Warning. Terr. Atmos. Ocean. Sci., 27, 819-824, doi: 10.3319/TAO.2016.07.28.02

1. INTRODUCTION

Earthquake early warning (EEW) systems are proven to be effective tools for real-time seismic hazard mitigation, and are operated in many countries, for instance, Taiwan, Japan, Mexico, and Southern California (Nakamura 1988; Aranda et al. 1995; Kanamori et al. 1997; Wu et al. 1999; Allen and Kanamori 2003; Kamigaichi 2004; Horiuchi et al. 2005; Zollo et al. 2006; Allen et al. 2009; Hsiao et al. 2009; Lee and Wu 2011; Satriano et al. 2011). EEW provides alerts to urban areas near the epicenter of a forthcoming strong ground shaking caused by large earthquakes that may affect sensitive facilities such as public transportation systems.

There are two approaches adopted for EEW systems: regional warning and on-site warning. In regional warning, the seismic records of the closer-to earthquake seismic sensors or network are used to predict strong ground motions at more distant regions. In on-site warning, the initial *P*-wave motion is used to predict the ground motions of later arriving *S* and surface waves, which commonly have higher amplitudes and destructive energy than that of the initial *P*-wave. Generally, the regional approach is more comprehensive and accurate, but it takes a longer time to produce results because it requires information from a number of stations. The on-site warning system has a shorter reporting time than the regional one, but the regional one has a higher accuracy than the on-site one because more stations are used, providing complete phase arrivals.

As an amplitude parameter, the peak amplitude of the initial 3-sec *P*-wave vertical displacement, P*d*, reflects the attenuation relationship of the ground motion with distance (Wu and Zhao 2006; Wu et al. 2006), which leads to practical applications for EEW. This suggests that we can estimate the earthquake magnitude once the epicentral distance and P*d* are available. When a large earthquake happens, its location can be quickly obtained from a few *P*-wave arrivals at nearby stations. P*d* can then be used to determine the magnitude via the attenuation relationship. The relationships between the earthquake magnitude and several characteristic parameters obtained in the first few seconds from the *P*-wave have been developed for EEW applications (Allen and Kanamori 2003; Wu and Kanamori 2005a, b; Wu and Zhao 2006; Hsiao et al. 2011).

Taiwan is located on the western portion of the Circum-Pacific seismic belt with a plate convergence rate of

* *Corresponding author*
E-mail: ljegay1111@gmail.com

8 cm per year. Earthquakes are both frequent and serious disasters in Taiwan. We considered P*d* from borehole seismic recording as an amplitude parameter for earthquake magnitude (M_{Pd}) determination for EEW. We defined a new robust P*d* regression equation for the Taiwan borehole seismic network.

2. SEISMIC NETWORK AND DATA

We acquired borehole seismographs from the Central Weather Bureau (CWB) borehole seismic network. The vertical acceleration signals were numerically double-integrated to obtain the displacements and filtered using a 0.075 Hz high-pass recursive Butterworth filter to remove the low-frequency drift after the last integration. P*d* is defined as the peak amplitude of filtered displacement during the initial 3 sec of *P*-waves. Since only the vertical motion component is used in this study, we assume that the vertical borehole seismometer component is well orientated and any deviation from this can be neglected (Krieger and Grigoli 2015; Wang et al. 2016; Zaldívar et al. 2016). The CWB has been installing the borehole seismometers since 2007. However, we selected events occurring after 2012 in this study to ensure stable network operation and data quality. Figure 1 shows the 29 stations used in this study. Each station has strong-motion seismographs installed at the free surface and bottom of the borehole with a depth range between 100 and 400 m. We used only the borehole data to reduce the receiver site near-surface effects and better extract the source signature registered in the initial *P*-wave arrival portion.

We selected in-land and offshore (distance to shoreline < 10 km) regional earthquakes from the CWB catalog that occurred between 2012 and 2014 with $M_L > 4.0$ and focal depths shallower than 50 km (Table 1). Most inland and inshore earthquakes that cause ground shaking to a maximum peak ground acceleration > 80 gal (1 gal = 1 cm s^{-2}) have focal depths shallower than 25 km in Taiwan. We further restricted the study to events that were recorded by a minimum of five stations (i.e., at least 5 P*d*), and there are a total of 68 events (Fig. 1) and 465 P*d* recordings.

3. RESULTS AND DISCUSSION

According to previous studies {Fowler 2004 [Eq. (4.13)]; Wu and Zhao 2006}, we assumed a linear regression model among the logarithmic P*d*. The CWB reported local magnitude M_L, and the logarithmic hypocentral distance *R*:

$$\log(\mathrm{P}d) = a + bM_L + c\log(R) \tag{1}$$

where *a*, *b*, and *c* are constants to be determined from the regression analysis.

Equation (1) can be rewritten in matrix form as:

$$\begin{bmatrix} \log \mathrm{P}d_1 \\ \log \mathrm{P}d_2 \\ \vdots \\ \log \mathrm{P}d_n \end{bmatrix}_{n\times 1} = \begin{bmatrix} 1 & M_{L_1} & \log(R_1) \\ 1 & M_{L_1} & \log(R_2) \\ \vdots & \vdots & \vdots \\ 1 & M_{L_m} & \log(R_n) \end{bmatrix}_{n\times 3} \cdot \begin{bmatrix} a \\ b \\ c \end{bmatrix}_{3\times 1} \tag{2}$$

where *n* and *m* are the numbers of recordings and events, respectively. Equation (2) presents a typical over-determined inversion problem and can be viewed as Gm = d. G and d are the data kernel and data vector, respectively. The vector of unknowns (model parameter vector: m) were found through standard least-squares solutions (Menke 1984; Miao and Langston 2007). Firstly, we used all 465 readings (n = 465) to obtain the initial parameter model. P*d* larger than twice the standard deviations of the expected value were then excluded from the data set. Next the remaining P*d* (n = 424) were used to invert the linear regression model [Eq. (3)]. The resulting best-fitting attenuation relationship for log(P*d*) is given by

$$\log(\mathrm{P}d) = 0.689M_L - 0.741\log(R) - 4.608 \pm 0.248 \tag{3}$$

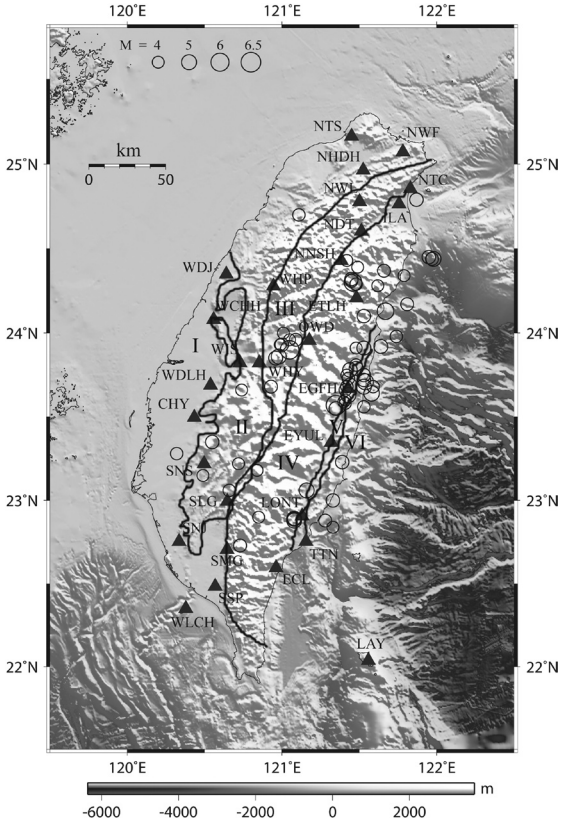

Fig. 1. Station distribution of the Taiwan borehole network and the epicenter locations of the 68 events used in this study. Geological provinces are indicated by the solid lines and denoted by I, the Coastal Plain; II, the Western Foothills; III, Hsuehshan Range; IV, Backbone Range; V, Longitudinal Valley; VI, Coastal Range. The Central Range is composed of two ranges, the Backbone Range in the east and the Hsuehshan Range in the west.

Table 1. Event information.

Origin	Time	Lat. (E)	Lon. (N)	Depth (km)	Magnitude (M_L)	Origin	Time	Lat. (E)	Lon. (N)	Depth (km)	Magnitude (M_L)
2012/02/18	01:33	23.68	121.59	21.4	4.3	2013/10/31	20:02	23.57	121.35	15.0	6.4
2012/04/19	09:58	24.13	121.67	29.1	5.5	2013/10/31	21:29	23.58	121.41	10.4	4.0
2012/04/28	05:08	22.73	120.73	24.0	4.4	2013/10/31	23:47	23.63	121.43	10.1	5.1
2012/05/31	14:58	24.39	121.49	5.2	4.1	2013/11/01	04:30	23.60	121.41	10.1	4.1
2012/06/14	12:07	23.72	121.53	6.2	4.5	2013/11/01	04:44	23.59	121.40	9.3	4.1
2012/06/15	00:15	23.71	121.54	6.5	5.3	2013/11/01	07:52	23.69	121.44	14.1	4.8
2012/06/17	17:01	23.68	121.53	6.5	5.0	2013/11/12	20:08	23.81	121.48	16.3	4.3
2012/11/05	21:40	23.78	121.44	14.1	4.9	2013/12/25	15:38	23.68	121.42	19.0	4.3
2013/01/03	22:37	23.98	121.74	7.0	4.3	2014/01/15	00:44	23.86	120.98	15.0	5.0
2013/01/17	16:30	24.44	121.98	13.7	5.1	2014/01/15	02:38	22.89	121.08	8.3	5.1
2013/02/06	19:58	24.10	121.53	21.2	4.5	2014/01/15	03:50	22.88	121.08	8.4	5.1
2013/02/17	09:32	24.32	121.45	6.3	4.6	2014/01/15	07:06	22.89	121.08	8.3	4.5
2013/02/19	10:12	23.35	120.55	15.1	4.6	2014/01/23	00:28	23.73	121.43	21.8	4.3
2013/02/20	23:20	23.23	121.39	20.0	4.5	2014/01/23	20:41	23.66	121.41	17.3	4.2
2013/02/22	02:33	24.31	121.45	5.3	4.4	2014/01/25	11:16	23.79	121.48	11.8	4.7
2013/03/04	16:42	23.00	121.33	23.7	4.6	2014/02/16	00:14	23.06	120.66	16.5	4.3
2013/03/06	19:49	24.44	121.97	13.4	4.4	2014/03/05	00:02	23.22	120.72	7.6	4.1
2013/03/07	11:36	24.30	121.46	5.6	5.9	2014/04/01	08:11	23.96	121.09	30.8	4.4
2013/03/13	11:51	24.17	121.81	9.8	4.4	2014/04/26	00:33	23.55	121.35	17.6	4.7
2013/03/17	21:53	23.68	120.93	12.3	4.4	2014/05/16	04:21	23.15	120.49	15.0	4.0
2013/03/20	15:22	24.45	121.95	12.1	4.6	2014/05/20	14:49	22.90	120.85	5.7	4.1
2013/03/27	10:03	23.90	121.05	19.4	6.2	2014/05/24	01:25	23.56	121.53	31.7	4.2
2013/03/27	11:30	23.93	121.00	14.0	4.5	2014/05/24	21:39	24.43	121.42	5.3	4.1
2013/03/28	02:46	23.93	120.99	13.1	4.0	2014/05/25	20:41	23.06	121.16	12.7	5.0
2013/04/15	13:57	24.29	121.48	7.1	4.2	2014/05/31	05:19	22.88	121.28	17.8	4.4
2013/05/19	08:20	24.37	121.66	58.9	4.4	2014/05/31	10:51	24.70	121.11	9.2	4.2
2013/05/30	11:14	23.92	121.64	46.9	4.8	2014/06/06	15:36	23.75	121.42	19.2	4.0
2013/06/20	23:11	23.91	121.48	15.1	4.1	2014/06/15	05:22	23.75	121.53	6.0	4.6
2013/06/26	18:19	24.79	121.87	10.0	4.5	2014/06/20	01:46	23.18	120.84	4.2	4.1
2013/06/30	12:57	24.00	121.01	16.3	4.1	2014/09/24	09:01	24.34	121.79	8.4	4.1
2013/07/06	12:17	22.84	121.33	21.2	4.1	2014/10/08	02:08	23.64	121.58	33.4	5.2
2013/07/15	23:01	23.96	121.05	19.1	4.0	2014/10/20	17:49	24.28	121.62	47.5	4.0
2013/07/24	22:47	23.91	121.53	9.1	4.8	2014/10/23	08:53	23.66	120.74	20.6	4.0
2013/09/30	20:05	23.85	120.96	11.1	4.7	2014/10/29	07:16	23.28	120.32	9.4	4.3

Equation (3) indicates that with hypotral distances and P*d* available the P*d* magnitudes, M_{Pd}, can be obtained as

$$M_{Pd} = 1.451 \log(Pd) + 1.076 \log(R) + 6.688 \quad (4)$$

M_{Pd} and M_L are both based on the amplitude attenuation with distance from the source.

Figure 2 shows the observed P*d* values compared with the values predicted by Eq. (3) separately for magnitudes of 4.5, 5.5, and 6.5. We used the average of all available M_{Pd} as the final magnitude for each event. For the real-time operation, the earthquake locations and M_{Pd} can be determined from the first couple of *P*-wave arrivals to reduce the P*d* collection time. In Fig. 3, we compared the CWB reported M_L to the M_{Pd}, and the resulting standard deviation between the reported M_L and the average M_{Pd} is of 0.21 ($M_{Pd} = M_L \pm 0.21$). This standard deviation is fairly acceptable in the EEW system.

In order to verify the borehole P*d* attenuation equation [Eq. (2)], we used P*d* values in our study to calculate M_{Pd} using Eq. (4) and the free-surface P*d* regression equation (Hsiao et al. 2011), respectively. Since the event magnitudes used in the study of Hsiao et al. (2011) are larger than 4.5, we only compared event magnitudes larger than 4.5. Figure 3 clearly suggests the necessity for a specific P*d* regression equation for the borehole data. Figure 3 shows that for larger events of about $M > 6.0$, M_{Pd} calculated by Hsiao et al. (2011) are closer to these using Eq. (4). This might imply that a larger magnitude event has longer period signal content (i.e., longer wavelength) than a smaller one in the early *P*-wave potion. This magnitude-dependent frequency characteristic is understood as the frequency-dependent source excitation (Hanks and Kanamori 1979). For a wave with a wavelength comparable to the borehole depth. The amplitude properties of the propagating wave between the

borehole and free surface should be more similar than those of a propagating wave with a shorter wavelength.

In the study of Hsiao et al. (2011), M_{Pd} estimated using the free-surface P*d* regression equation has a 1:1 relationship with the CWB catalog M_L with a standard deviation of 0.43. The borehole record application in M_{Pd} in theory should be more robust due to the reduced near surface effect caused by the low shear-wave velocity, low quality factor (Q), or topographic effect. The smaller standard deviation of 0.21 presented in Eq. (4) than that of Hsiao et al. (2011) might be attributed to the reduced influence of the near-surface effect in the borehole records to some extent.

The site effect is one of the important factors that affects ground motion prediction. We determined the P*d* site correction (S) by averaging the residuals between the observed and predicted values as follows (Wu et al. 2001):

$$S = \exp\left(\frac{1}{n}\sum_{i=1}^{n} \ln \frac{Pd_{obs.}}{Pd_{pre.}}\right) \quad (5)$$

where n is amount of P*d* for the corresponding station. The total amount of $Pd_{obs.}$ is 669 from the events that were recorded by at least three stations. Figure 4 presents the resulting S

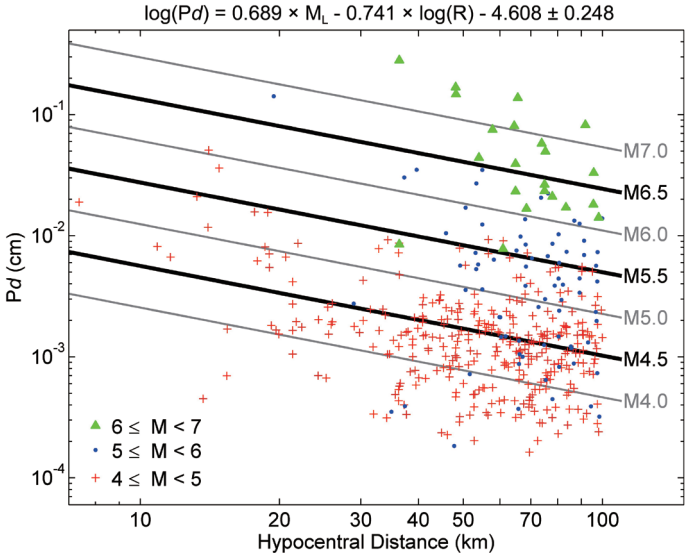

Fig. 2. Distribution of the 424 observed P*d* measurements. The predicted curves by Eq. (3) are depicted by the solid lines for a variety of magnitudes from 4.0 - 7.0. (Color online only)

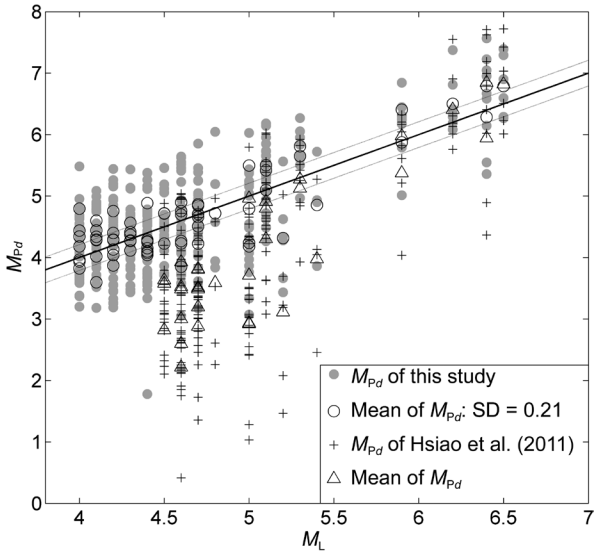

Fig. 3. Magnitudes (M_{Pd}) determined from P*d* versus the CWB reported M_L. Solid line shows the least squares fit for the mean of M_{Pd} and two dashed lines show the range of one standard deviation.

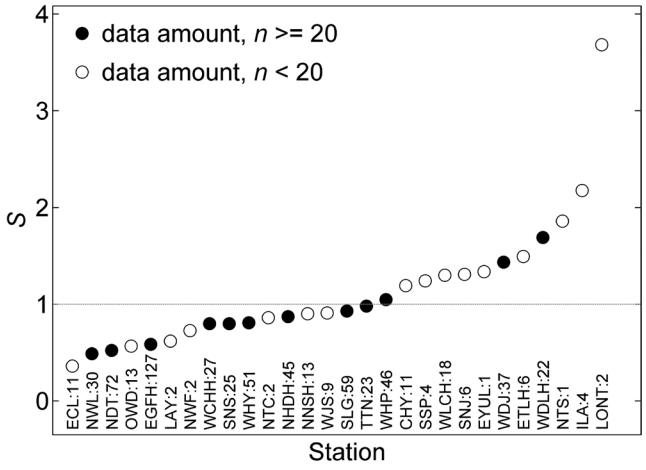

Fig. 4. Site correction (*S*) for the borehole P*d* observations at each station.

for each borehole station. The largest *S* with $n > 20$ was found at the WDLH station on the Coastal Plain, which has the lowest near-surface Vs (427 ± 29 m s^{-1}), the highest Qp (38 ± 14), and the third highest Vp/Vs ratio (4.24) among the borehole stations in Taiwan (Wang et al. 2016). The low near-surface Vs, high Qp, and high Vp/Vs suggest near-surface unconsolidated soil and high pore-fluid content beneath the WDLH station. The smallest *S* with $n > 20$ was found at the NWL station in the Central Mountain Range. In contrast to the WDLH station, the NWL station has the highest Vp (3752 m s^{-1}) and Vs (2056 m s^{-1}) (Wang et al. 2016).

Since the Taiwan borehole network recording period is very short compared to free-surface ground motion observations, only 12 stations out of 29 stations (41%) had quality P*d* recordings greater than 20. The standard deviation of the free-surface P*d* regression equation (Hsiao et al. 2011) is larger than that derived using the borehole P*d* values in this study. Therefore, it might not be so encouraging to use the P*d* regression equation for surface sensors incorporated with the borehole P*d* site effect as another approach to bring the borehole data into the routine EEW operation.

Acknowledgements The waveform data were requested from the Central Weather Bureau (CWB). We greatly appreciate the CWB for providing data. The GMT (Wessel and Smith 1998) software program was used in this study and is gratefully acknowledged. This study was supported by the Ministry of Science and Technology of Taiwan (MOST 104-2116-M-006-003). Two Anonymous Reviewers are gratefully acknowledged for their comments on this manuscript.

REFERENCES

Allen, R. M. and H. Kanamori, 2003: The potential for earthquake early warning in southern California. *Science*, **300**, 786-789, doi: 10.1126/science.1080912. [Link]

Allen, R. M., P. Gasparini, O. Kamigaichi, and M. Böse, 2009: The status of earthquake early warning around the World: an introductory overview. *Seismol. Res. Lett.*, **80**, 682-693, doi: 10.1785/gssrl.80.5.682. [Link]

Aranda, J. M. E., A. Jiménez, G. Ibarrola, F. Alcantar, A. Aguilar, M. Inostroza, and S. Maldonado, 1995: Mexico City seismic alert system. *Seismol. Res. Lett.*, **66**, 42-53, doi: 10.1785/gssrl.66.6.42. [Link]

Fowler, C. M. R., 2004: The Solid Earth: An Introduction to Global Geophysics, Cambridge University Press, New York, 728 pp, doi: 10.1017/CBO9780511819643. [Link]

Hanks, T. C. and H. Kanamori, 1979: A moment magnitude scale. *J. Geophys. Res.*, **84**, 2348-2350, doi: 10.1029/JB084iB05p02348. [Link]

Horiuchi, S., H. Negishi, K. Abe, A. Kamimura, and Y. Fujinawa, 2005: An automatic processing system for broadcasting earthquake alarms. *Bull. Seismol. Soc. Am.*, **95**, 708-718, doi: 10.1785/0120030133. [Link]

Hsiao, N. C., Y. M. Wu, T. C. Shin, L. Zhao, and T. L. Teng, 2009: Development of earthquake early warning system in Taiwan. *Geophys. Res. Lett.*, **36**, L00B02, doi: 10.1029/2008GL036596. [Link]

Hsiao, N. C., Y. M. Wu, L. Zhao, D. Y. Chen, W. T. Huang, K. H. Kuo, T. C. Shin, and P. L. Leu, 2011: A new prototype system for earthquake early warning in Taiwan. *Soil Dyn. Earthq. Eng.*, **31**, 201-208, doi: 10.1016/j.soildyn.2010.01.008. [Link]

Kamigaichi, O., 2004: JMA earthquake early warning. *J. JAEE*, **4**, 134-137, doi: 10.5610/jaee.4.3_134. [Link]

Kanamori, H., E. Hauksson, and T. Heaton, 1997: Real-time seismology and earthquake hazard mitigation. *Nature*, **390**, 461-464, doi: 10.1038/37280. [Link]

Krieger, L. and F. Grigoli, 2015: Optimal correction of data from misoriented multi-component geophysical sensors. The 19th International Symposium on Recent

Advances in Exploration Geophysics (RAEG 2015), 6 pp, doi: 10.3997/2352-8265.20140191. [Link]

Lee, W. H. K. and Y. M. Wu, 2011: Earthquake monitoring and early warning systems. In: Meyers, R. A. (Ed.), Extreme Environmental Events: Complexity in Forecasting and Early Warning, Springer, New York, 278-311, doi: 10.1007/978-1-4419-7695-6_18. [Link]

Miao, Q. and C. A. Langston, 2007: Empirical distance attenuation and the local-magnitude scale for the central United States. *Bull. Seismol. Soc. Am.*, **97**, 2137-2151, doi: 10.1785/0120060188. [Link]

Menke, W., 1984: Geophysical Data Analysis: Discrete Inverse Theory, Academic Press Inc, Orlando, Florida, 260 pp.

Nakamura, Y., 1988: On the urgent earthquake detection and alarm system (UrEDAS). Proceedings of the Ninth World Conference on Earthquake Engineering, Vol. 7, 673-678.

Satriano, C., Y. M. Wu, A. Zollo, and H. Kanamori, 2011: Earthquake early warning: Concepts, methods and physical grounds. *Soil Dyn. Earthq. Eng.*, **31**, 106-118, doi: 10.1016/j.soildyn.2010.07.007. [Link]

Wang, Y. J., K. F. Ma, S. K. Wu, H. J. Hsu, and W. C. Hsiao, 2016: Near-surface attenuation and velocity structures in Taiwan from wellhead and borehole recordings comparisons. *Terr. Atmos. Ocean. Sci.*, **27**, 169-180, doi: 10.3319/TAO.2015.10.07.01(T). [Link]

Wessel, P. and W. H. F. Smith, 1998: New, improved version of Generic Mapping Tools released. *Eos, Trans., AGU*, **79**, 579, doi: 10.1029/98EO00426. [Link]

Wu, Y. M. and H. Kanamori, 2005a: Experiment on an onsite early warning method for the Taiwan early warning system. *Bull. Seismol. Soc. Am.*, **95**, 347-353, doi: 10.1785/0120040097. [Link]

Wu, Y. M. and H. Kanamori, 2005b: Rapid assessment of damage potential of earthquakes in Taiwan from the beginning of *P* waves. *Bull. Seismol. Soc. Am.*, **95**, 1181-1185, doi: 10.1785/0120040193. [Link]

Wu, Y. M. and L. Zhao, 2006: Magnitude estimation using the first three seconds P-wave amplitude in earthquake early warning. *Geophys. Res. Lett.*, **33**, L16312, doi: 10.1029/2006GL026871. [Link]

Wu, Y. M., J. K. Chung, T. C. Shin, N. C. Hsiao, Y. B. Tsai, W. H. K. Lee, and T. Teng, 1999: Development of an integrated earthquake early warning system in Taiwan-case for the Hualien area earthquakes. *Terr. Atmos. Ocean. Sci.*, **10**, 719-736.

Wu, Y. M., T. C. Shin, and C. H. Chang, 2001: Near real-time mapping of peak ground acceleration and peak ground velocity following a strong earthquake. *Bull. Seismol. Soc. Am.*, **91**, 1218-1228, doi: 10.1785/0120000734. [Link]

Wu, Y. M., H. Y. Yen, L. Zhao, B. S. Huang, and W. T. Liang, 2006: Magnitude determination using initial *P* waves: A single-station approach. *Geophys. Res. Lett.*, **33**, L05306, doi: 10.1029/2005GL025395. [Link]

Zaldívar, E. R. D., E. Priolo, F. Grigoli, and S. Cesca, 2016: Misalignment angle correction of borehole seismic sensors: The case study of the Collalto seismic network. *Seismol. Res. Lett.*, **87**, 668-677, doi: 10.1785/0220150183. [Link]

Zollo, A., M. Lancieri, and S. Nielsen, 2006: Earthquake magnitude estimation from peak amplitudes of very early seismic signals on strong motion records. *Geophys. Res. Lett.*, **33**, L23312, doi: 10.1029/2006GL027795. [Link]